DUCTILE FRACTURE UNDER MULTIAXIAL STRESS STATES BETWEEN PAIRS OF HOLES

R. J. Bourcier and D. A. Koss
Department of Metallurgical Engineering
Michigan Technological University
Houghton, Michigan 49931 U.S.A.

ABSTRACT

As a means of examining ductile fracture under multiaxial stress and strain states, the deformation and fracture between pairs of holes has been studied in a 7075 Aℓ alloy. The test technique, which is unique, utilizes tensile samples each with a pair of holes through the thickness. The holes are sufficiently close (two hole diameters apart) so as to concentrate slip between them, and the local states of stress and strain can be controlled by the orientation of the holes to the stress axis.

The influence of hole orientation on the strain at fracture has been determined in the 7075 Aℓ alloy in the T6 as well as TO tempers. Fracture occurs by flow localization between the holes and very little hole growth occurs, especially in the T6 condition. Fractography indicates a transition in fracture appearance with hole orientation with dimpled fracture predominating, but the degree of shear fracture increases as the pair of holes become more inclined to the stress axis. A modification of the Bridgeman analysis is used as a description of the approximate state of stress between the holes as a function of the hole orientation. The results indicate that the criterion for ductile fracture depends on both the state of stress and the strain state, but the functional dependence could not be determined. The results are also discussed as a model for void coalescence in ductile fracture and suggest the importance of flow instability in the void link-up process.

KEYWORDS

Ductile fracture; multiaxial stress states; holes and voids; fracture criteria; 7075 Aℓ alloy.

INTRODUCTION

Ductile fracture cannot be fully understood until its functional dependence on stress as well as strain states is established. In recent years, many studies have analyzed ductile fracture on a microscopic scale using void initiation and void growth processes based on dislocation models, continuum plasticity analyses, and experimental studies of soft, ductile alloys (for reviews, see Mogford, 1967; Rosenfield, 1968; McClintock, 1968 and 1971; and Goods and Brown, 1979). From a

macroscopic standpoint, the importance of the hydrostatic or mean stress on ductile fracture is well established (Bridgeman, 1952 and Pugh, 1967). However, there have been relatively few experimental efforts to establish macroscopic criteria for ductile fracture occurring under multiaxial stress and strain states (Hancock and Mackenzie, Hancock, and Brown, 1977; and Osakeda, Watadani, and Sekiguchi, 1977). As a means of establishing ductile fracture criteria under multiaxial stress conditions and of modeling void link-up in the ductile fracture of high strength alloys, the present research examines deformation and fracture between pairs of holes. The test technique, which is unique, utilizes tensile samples each with a pair of holes drilled through the thickness. The holes are sufficiently close (two hole diameters apart) so as to concentrate slip between them, and the local strain components are measured with the aid of a square grid of lines. The orientation of the holes to the tensile axis can be systematically varied, and thus the states of stress and strain between the holes may be controlled. Fracture of the tensile sample occurs when the ligament between the holes fails. A series of tests as a function of hole orientation therefore permits one to subject the material in the ligament between the holes to different stress states and to measure the state of strain at fracture. The observed behavior also contains implications regarding void link-up, and these will be discussed. Results are presented for a 7075 Aℓ alloy both in the T6 and TO tempers.

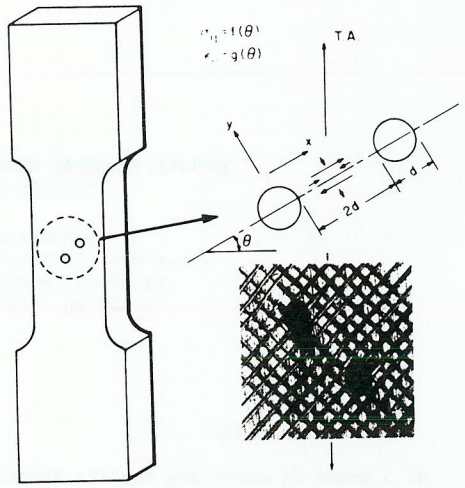

Fig. 1. A schematic diagram of the pair-of-holes tensile sample. Note that the holes are centrally located in a gauge section ≃25 d wide and ≃75 d long. The insert is a photomicrograph showing a pair of holes at θ ≃ 45° and at a strain near fracture.

EXPERIMENTAL PROCEDURE

The experimental data is obtained using a pair of holes tensile sample shown in Fig. 1. In this study, the holes in Fig. 1 are 0.5mm diameter, the centers of the holes are 1.5mm apart, and they are drilled through a gauge section 6.4mm thick and 12.8mm wide. A square grid of lines spaced ∿0.4mm apart was scribed onto the sample such that the grid axes correspond to the x and y axes in Fig. 1. All tests were performed at a constant displacement rate such that the nominal engineering strain rate was .005 sec^{-1}.

The presence of the grids and the initial dimensions of the section of the sample containing the holes permits an accurate determination of the average state of strain in the ligament between the holes. In terms of the axes in Fig. 1, the shear strain γ_{xy} can be measured directly from the grid at any time prior to fracture. The normal strain components ε_{xx} and ε_{zz} (see Fig. 1 for definition of axes) are measured by recording edge to edge spacings of the holes along the center to center plane between the holes during the test (which yields ε_{xx}) and by measuring the thickness of the ligament before and after fracture (from which ε_{zz} at fracture is determined). Macrophotography is used to determine ε_{xx} and γ_{xy} prior to fracture. As expected, these strain components are linearly dependent on tensile strain. Therefore the state of strain at fracture is obtained by measuring ε_{xx} and γ_{xy} periodically as a function of tensile strain and extrapolating a small amount (<1% strain) to the tensile fracture strain ε_f of the specimen. The third normal strain component in the plane of the fracture, ε_{yy}, is then calculated by assuming constant volume.

The material used in this study was a 7075 Aℓ alloy (in wt. %: 1.60 Cu, 2.46 Mg, 5.78 Zn, .26 Fe, .19 Cr, and .10 Si) obtained courtesy of the Aluminum Corporation of America in the form of 6.4mm thick plate. After specimen preparation according to Fig. 1, the samples were heat treated to either the T6 temper (solution-treated at 465°C for three hours, water quenched, and aged at 120°C for twenty-four hours) or a TO temper (425°C for 1 hour, furnace cool at 28°C/hr to 230°C plus 6 hours at 230°C). In both cases, the grain size is approximately 0.1mm.

EXPERIMENTAL RESULTS

The dependence of the tensile strain and the strain components at the point of fracture of the ligament between the holes on the hole orientation is shown in Fig. 2 (T6 temper) and Fig. 3 (TO temper). It should be noted that the schematic insert in Figs. 2 and 3 depicting the sample is not drawn to scale as in reality the holes are located ≃10 hole diameters from the sides of the gauge section.

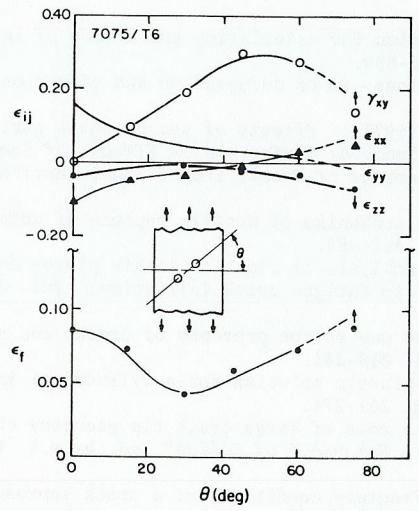

Fig. 2. The dependence of the strain components ε_{ij} at fracture of the ligament between the holes and of the tensile strain to fracture ε_f on hole orientation θ for a 7075 Aℓ alloy in the T6 temper. The magnitude of ε_f is based on the central section of the gauge length, ∿15 d long, containing the pair of holes.

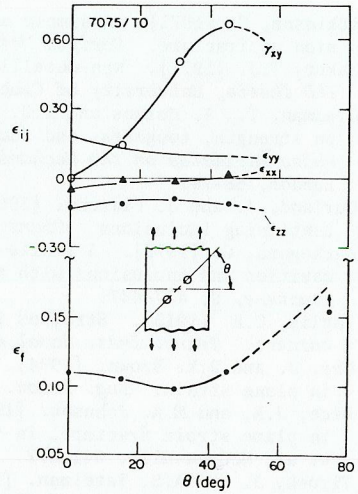

Fig. 3. The dependence of the strain components ε_{ij} at fracture of the ligament between the holes and of the tensile strain to fracture ε_f on hole orientation θ for a 7075 Aℓ alloy in the TO temper.

Figures 2 and 3 clearly indicate that the strain components ε_{ij} at fracture are strongly dependent on hole orientation with a transition occurring from a state of strain characterized by normal strains at $\theta = 0°$ to predominantly a single shear strain component γ_{xy} $(= \gamma_{yx})$ at $\theta = 45°$. The tensile strain to fracture ε_f [based on the central section of the gauge length, ~15 hole diameters long, which contains the holes] is also very dependent on hole orientation, showing a minimum at $\theta = 30°$ for both tempers, see Figs. 2 and 3. This behavior occurs not only in the 7075 Aℓ alloy tested here, but also in 1.5mm thick Ti-8Aℓ-1Mo-1V sheet tested with the pairs of holes sample configuration.

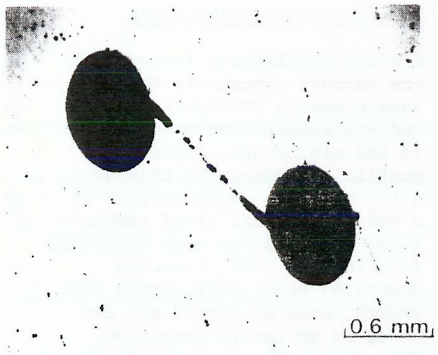

Fig. 4. An optical micrograph showing the profile of a sheet of voids forming prior to fracture of the ligament between the pair of holes in a 7075 Aℓ alloy in the TO temper. The tensile axis is vertical.

Figure 4 shows a profile of the ligament just prior to macroscopic fracture. Relatively little hole growth occurs prior to fracture, especially in the T6 condition (note: Fig. 4 is of the TO condition which failed more gradually, enabling this micrograph to be obtained). Figure 4 also shows the formation of voids between the holes and suggests their link-up by a shear process. As such, Fig. 4 is very similar to the classic micrographs of Cox and Low (1974) and Forsythe and Smale (1971) showing void link-up in a 4340 steel and BSL 64 Aℓ, respectively. Examination of the fracture surface profiles between the holes in other TO and T6 samples indicate that fracture at $\theta \leq 60°$ occurs on a plane similar to that being developed in Fig. 4. This plane is close to but not identical with the plane connecting the axes of the holes.

Fractography indicates a transition in fracture appearance with hole orientation. At $\theta = 0°$ (i.e., holes oriented perpendicular to the stress axis), the fracture surface is characterized by void formation and coalescence typical of tensile fracture. The dimples are elongated parallel to the plate surface, and inclusions, also typical of 7075 Aℓ. However, beginning with the $\theta = 15°$ samples, the fracture surfaces also contain regions of shear-type fracture in addition to the dimpled fracture. The extent of the shear areas increases with increasing θ from about 20% at $\theta = 15°$ to a maximum of about 40% of the fracture surface at $\theta = 60°$ in the T6 sample. While the $\theta \neq 0°$ samples fail by mixed mode I and mode II displacements, the dimples present in the inclined-hole fracture surfaces are not significantly elongated in the shear direction.

DISCUSSION

Stress and Strain States Between the Holes

Any analysis of the experimental data must recognize the multiaxial nature of both the strain state and stress state. The nature of the test is such that, although the condition of plane strain nearly prevails in the T6 material, fracture between the holes occurs under neither plane stress nor, strictly speaking, plane strain. The equivalent plastic strain in the ligament at fracture can be calculated directly from the experimental plastic strain components ε_{ij} and is:

$$\bar{\varepsilon}_f = \left| \frac{2}{9} \{(\varepsilon_{xx}-\varepsilon_{yy})^2 + (\varepsilon_{yy}-\varepsilon_{zz})^2 + (\varepsilon_{zz}-\varepsilon_{xx})^2\} + \frac{1}{3}\gamma_{xy}^2 \right|^{\frac{1}{2}} \qquad (1)$$

Determination of the state of stress in the ligament at fracture presents considerably more difficulty. To do this, we assume that the Bridgeman analysis (1952) for the stress state* in a necked tensile specimen can be modified by resolving the nominal axial stress σ_a on the present test sample into a shear stress component σ_{xy} and the normal stresses σ_{yy} and σ_{xx}. The stress state in the ligament between the holes can be roughly estimated by taking into account the reduced area of this section and by assuming that the σ_{yy} component $(\sigma_a \cos^2\theta)$ generates triaxial stresses in the ligament according to the Bridgeman analysis (1952). Assuming plane strain, this analysis gives the following crude estimate of the normal stresses between a pair of holes of radius R and whose surfaces are spaced 2a apart in a gauge section W wide:

$$\left.\begin{aligned} & \sigma_{xx} \gtrsim \sigma^* \cos^2\theta \; \ell n\, A \\ \text{but} \quad & \sigma_{xx} \lesssim \sigma^* \cos^2\theta \; \ell n\, A + \sigma_a \sin^2\theta \\ & \sigma_{yy} \simeq \sigma^* \cos^2\theta [1+\ell n\, A] \;, \quad \sigma_{zz} = \tfrac{1}{2}(\sigma_{xx} + \sigma_{yy}) \\ & \sigma_{xy} \simeq \left(\frac{W}{W-4R\cos\theta}\right) \sigma_a \cos\theta \sin\theta \\ \text{and} \quad & \sigma_{xz} = \sigma_{yz} = 0 \;, \quad \text{where } A = 1 + \frac{1}{2}\frac{a}{R}\left(1 - \frac{x^2}{a^2}\right) \\ \text{and} \quad & \sigma^* = \left(\frac{W}{W-4R\cos\theta}\right) \frac{\sigma_a}{\{(1+\frac{2R}{a})^{\frac{1}{2}} \ell n [1+\frac{a}{R}+(\frac{2a}{R})^{\frac{1}{2}}(1+\frac{a}{2R})^{\frac{1}{2}}]-1\}} \end{aligned}\right\} \qquad (2)$$

In the present case, the pair of holes geometry is such that a/R = 2 in eqns. 2. The σ_{xx} component reflects the fact that, far from the holes (y >> 0), the term

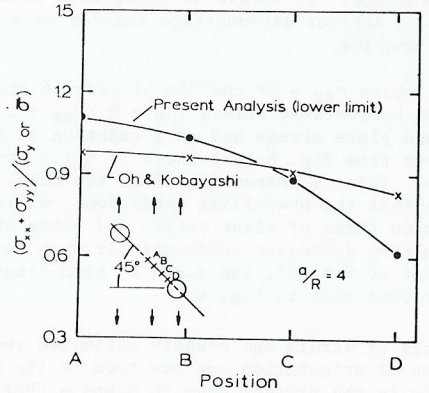

Fig. 5. The stress ratio $(\sigma_{xx} + \sigma_{yy})/(\sigma_y$ or $\bar{\sigma})$ as a function of the position between a pair of holes for the specific condition illustrated. The present analysis is based on $\sigma_{xx} = \sigma^* \cos^2\theta \; \ell n\, A$ with σ^* being calculated at the yield stress of the gauge section away from the holes (i.e., $\sigma_a = \sigma_y$). The Oh and Kobayashi (1976) data is at 10% strain in the ligament between the holes and is also for 7075 Aℓ/T6.

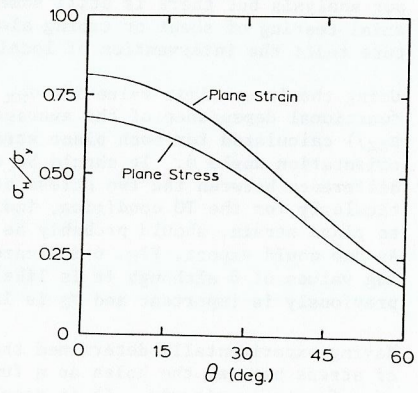

Fig. 6. The average value of σ_H/σ_y between a pair of holes as a function of hole orientation for conditions of plane strain vs. plane stress. The curves are calculated using the modified Bridgeman analysis (1952) described in the text using the lower limit value for σ_{xx} and at $\sigma_a = \sigma_y$. The plane stress values are based on $\sigma_{zz} = \sigma^* \cos^2\theta \; \ell n\, A$, using Bridgeman's relationship for σ_{zz}. Note that $(\ell n\, A)_{Ave}$ = 0.493 for a/R = 2.

*Clausing (1969) has modified Bridgeman's original work, but for the circular configuration and hole geometry used here the values of $\sigma_H/\bar{\sigma}$ as determined by the two analyses should be within ≲ 20% of each other.

($\sigma_a \sin^2\theta$) exists because of the rotation of the stress axis. While there is some contribution to σ_{xx} between the holes from this term, especially as $\theta \to 90°$, that contribution must be less than $\sigma_a \sin^2\theta$ since $\sigma_{xx} = 0$ at $x = a$ and $y = 0$.

There is support for the use of eqns. 2 to describe roughly the stress state between the holes. In Fig. 5, the lower limit of the present analysis (i.e., $\sigma_{xx} = \sigma^* \cos^2\theta \ell n\, A$) is compared to the specific plane strain case analyzed by Oh and Koboyashi (1976). Finite element techniques were used to determine the stress-strain states between an array of holes at $\theta = 45°$ for holes spaced 4 hole diameters apart in which case the $(W/(W-4R\cos\theta))$ term is 1.25. Unfortunately, no other orientations were examined. The calculations for $\theta = 45°$ predict the presence of a shear band connecting the two holes as well as the hydrostatic tension ratio graphed in Fig. 5. This figure shows the present analysis is in good agreement (<10%) with the ratio of $(\sigma_{xx} + \sigma_{yy})/\bar{\sigma}$ calculated by Oh and Koboyashi except near the surface of the hole where present analysis significantly underestimates (∿25%) the stress ratio calculated by Oh and Koboyashi (1976). Under these conditions, Oh and Koboyashi calculate the average equivalent stress in the ligament $\bar{\sigma}$ to be $\bar{\sigma} \simeq 1.30\ \sigma_y$ (the yield stress) while the present analysis predicts $\bar{\sigma} = 1.25\ \sigma_y$. It is interesting to note that both analyses yield the same $((\sigma_{xx} + \sigma_{yy})/\sigma)_{Ave}$ ratio of 0.93. We thus conclude that at $\theta = 45°$ and probably for $0 \leq \theta \lesssim 60°$, eqns. 2 provide a reasonable estimate of the stress state if $\sigma_{xx} \simeq \sigma^* \cos^2\theta \ell n\, A$.

An obvious disadvantage of the present test as a multiaxial stress test is that, as seen in Fig. 5, the stress between holes is a function of position. The Oh and Koboyashi calculations show that the dependence on position is not as pronounced as our analysis but there is still some dependence. It should be recognized that multiaxial testing of sheet or tubing also has a serious disadvantage insofar as a fracture test: the intervention of localized necking.

Using the lower limit value for σ_{xx} (for which $\sigma_{zz} = \sigma^* \cos^2\theta \ell n\, A$), Fig. 6 shows the functional dependence of the average mean hydrostatic stress ($\sigma_H = \frac{1}{3}(\sigma_{xx} + \sigma_{yy} + \sigma_{zz})$) calculated for both plane strain and plane stress and as a function of hole orientation angle θ. It should be obvious from Fig. 6 that there is not a great difference between the two stress states. This is reassuring since the data, particularly for the TO condition, indicate that the prevailing conditions, while close to plane strain, should probably be between those of plane strain and plane stress. As one would expect, Fig. 6 indicates that σ_H decreases substantially with increasing values of θ although it is likely that at $\theta = 60°$, the $\sigma_a \sin^2\theta$ term ignored previously is important and σ_H is larger than that in Fig. 6.

Having experimentally determined the state of strain and crudely estimated the state of stress between the holes as a function of orientation, we now turn to the question of a fracture criteria. It is reasonable in the present case to suppose that ductile fracture might occur in the ligament between the holes at a critical combination of equivalent plastic strain $\bar{\varepsilon}_f$ and the hydrostatic stress state parameter $\sigma_H/\bar{\sigma}$ at failure initiation. Figure 7 shows the functional dependence of $\bar{\varepsilon}_f$, $\sigma_H/\bar{\sigma}$, as well as the tensile strain to fracture ε_f. Careful examination of Fig. 7 indicates that the data does not fit any obvious simple fracture criteria. Clearly the data does not fit either a critical hydrostatic stress or critical strain criteria. Nor can fracture criteria based on either a product: $(\sigma_H/\bar{\sigma})^a \cdot (\bar{\varepsilon}_f)^b$ or the sum: $A(\sigma_H/\bar{\sigma}) + B\,\bar{\varepsilon}_f$ to explain the experimental results. Equally unsuccessful are attempts to use the analysis of McClintock (1966, 1968) for fracture by hole growth and coalescence to explain the observed dependence of fracture strain on hole orientation. Thus, we conclude that there is no apparent fracture criteria which adequately predicts ductile fracture in the ligament between the holes.

Microscopic Considerations

Certain qualitative features of the failure process in the test sample appear straightforward and are significant with regard to the microscopic aspects of ductile fracture. In this Aℓ alloy which is characterized by a relatively high yield strength (∿520 MPa) and low work hardening ($d\ell n\sigma/d\ell n\varepsilon \cong .09$), fracture occurs by relatively little hole growth, even at $\theta = 0°$ and especially in the T6 condition. This is readily apparent in Fig. 4 which shows a sample in the much more ductile TO condition ($\sigma_y \simeq$ 110 MPa and $d\ell n\sigma/d\ell n\varepsilon \simeq .10$). Somewhat similar behavior has been observed in the tensile testing of perforated mild steel sheet. To the extent that these tests model the void link-up process in ductile fracture, this result indicates the potential importance of the link-up of voids by a shear process involving flow localization. That ductile fracture occurs by the possible intervention of plastic instability before complete homogeneous growth and coalescence of holes has also been recognized by others (Thomason, 1974).

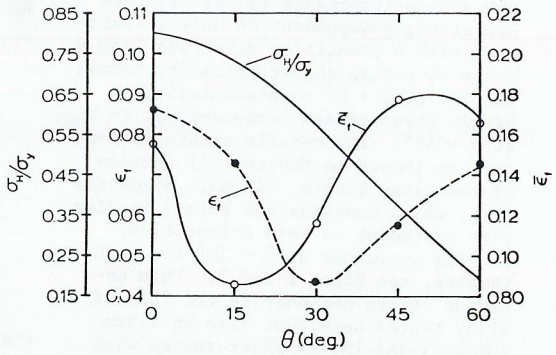

Fig. 7. The dependence of the stress ratio $\sigma_H/\bar{\sigma}$, the tensile strain to fracture ε_f, and the equivalent strain to fracture $\bar{\varepsilon}_f$ on the hole orientation θ for a 7075 Aℓ alloy in the T6 temper.

The sequence of events leading to failure is also clearly indicated. This sequence appears to be very similar to the void sheet process originally proposed by Rogers (1960) and based on microscopic observations of ductile fracture in copper. Upon straining to a point near fracture, voids form between the holes as shown in Fig. 4. Fracture in the ligament between the holes occurs when the "sheet" of voids is linked by a flow localization and shear process, giving rise to the shear fracture regions observed fractographically. Relatively little macroscopic strain occurs between the initiation of the large voids and their subsequent link-up by shear especially in the T6 condition.

SUMMARY

A test technique utilizing tensile samples with pairs of through-thickness holes has been described. This simple test may be utilized to study ductile fracture under a relatively broad combination of multiaxial stress as well as strain states. The corresponding stress state in the ligament between the holes can be reasonably estimated using a modified Bridgeman analysis while the state of strain can be determined experimentally. Results from tests performed on a 7075 Aℓ alloy indicate that fracture occurs by flow localization between the pair of holes with very little hole growth occurring prior to fracture. This macroscopic fracture process appears to be very similar to the microscopic void sheet mechanism. Although ductile fracture clearly depends on both the state of stress as well as the strain state, attempts to establish a well defined fracture criteria were unsuccessful. The results also suggest the importance of the link-up of voids by a shear localization process, as opposed to exclusively void growth and coalescence, in the ductile fracture of high strength alloys.

ACKNOWLEDGEMENTS

The authors would like to thank Mr. K. Chan and Dr. R. Tait for helpful discussions. This program was supported by the Office of Naval Research through Contract No. N00014-76-C-0037.

REFERENCES

Bridgeman, P. W. (1952). Studies in Large Plastic Flow and Fracture. McGraw-Hill, New York.
Clausing, D. P. (1969). J. Mat'l. JMLSA 4, 566.
Cox, T. B. and J. R. Low (1974). Met. Trans. 5, 1457.
Forsythe, P. J. E. and A. C. Smale (1971). Eng. Frac. Mech. 3, 127.
Goods, S. H. and L. M. Brown (1979). Acta Met., 27, 1.
Hancock, J. W. and A. C. Mackenzie (1976). J. Mech. Phys. Solids 24, 147.
Mackenzie, A. C., J. W. Hancock, and D. K. Brown (1977). Eng. Frac. Mech. 9, 167.
McClintock, F. A., S.M. Kaplan, and C. A. Berg (1966). Int. J. Frac. Mech. 2, 614.
McClintock, F. A. (1968). In Ductility, ASM: Metals Park, p. 255.
McClintock, F. A. (1968). J. Appl. Mech. 35, 363.
McClintock, F. A. (1971). In Fracture, Academic Press: New York, p. 47.
Mogford, I. L. (1967). Met. Rev. 12, 49.
Nagumo, M. (1973). Acta Met. 21, 1661.
Oh, S. I. and S. Koboyashi (1976). Theories of Flow and Fracture in Metalworking Processes, Air Force Materials Lab. Report AFML-TR-76-61, p. 61.
Osakada, K., A. Watadani and H. Sekiguchi (1977). Bull. Jap. Soc. Mech. Eng., 20, 1557.
Pugh, H. Ll. (1965). Irreversible Effects of High Pressure and Temperature on Materials, ASTM STP 374, ASTM, Philadelphia, p. 68.
Rogers, H. C. (1960). Trans. TMS-AIME 218, 498.
Rosenfield, A. R. (1968). Met. Rev. 13, 29.
Thomason, P. F. (1974). Prospects of Fracture Mechanics. Nordhoff Int. Pub.: Holland, p. 3.